NEOPLASIA
www.neoplasia.com

Volume 16 Number 9 September 2014 pp. 757–769 757

Synergistic Signaling of KRAS and Thyroid Hormone Receptor β Mutants Promotes Undifferentiated Thyroid Cancer through MYC Up-Regulation[1,2]

Xuguang Zhu, Li Zhao, Jeong Won Park, Mark C. Willingham and Sheue-yann Cheng

Laboratory of Molecular Biology, Center for Cancer Research, National Cancer Institute, National Institutes of Health, Bethesda, MD 20892, US

Abstract

Undifferentiated thyroid carcinoma is one of the most aggressive human cancers with frequent RAS mutations. How mutations of the *RAS* gene contribute to undifferentiated thyroid cancer remains largely unknown. Mice harboring a potent dominant negative mutant thyroid hormone receptor β, TRβPV ($Thrb^{PV/PV}$), spontaneously develop well-differentiated follicular thyroid cancer similar to human cancer. We genetically targeted the $Kras^{G12D}$ mutation to thyroid epithelial cells of $Thrb^{PV/PV}$ mice to understand how $Kras^{G12D}$ mutation could induce undifferentiated thyroid cancer in $Thrb^{PV/PV}Kras^{G12D}$ mice. $Thrb^{PV/PV}Kras^{G12D}$ mice exhibited poorer survival due to more aggressive thyroid tumors with capsular invasion, vascular invasion, and distant metastases to the lung occurring at an earlier age and at a higher frequency than $Thrb^{PV/PV}$ mice did. Importantly, $Thrb^{PV/PV}Kras^{G12D}$ mice developed frequent anaplastic foci with complete loss of normal thyroid follicular morphology. Within the anaplastic foci, the thyroid-specific transcription factor paired box gene 8 (PAX8) expression was virtually lost and the loss of PAX8 expression was inversely correlated with elevated MYC expression. Consistently, co-expression of $KRAS^{G12D}$ with TRβPV upregulated MYC levels in rat thyroid pccl3 cells, and MYC acted to enhance the TRβPV-mediated repression of the *Pax8* promoter activity of a distant upstream enhancer, critical for thyroid-specific *Pax8* expression. Our findings indicated that synergistic signaling of $KRAS^{G12D}$ and TRβPV led to increased MYC expression. Upregulated MYC contributes to the initiation of undifferentiated thyroid cancer, in part, through enhancing TRβPV-mediated repression of the *Pax8* expression. Thus, MYC might serve as a potential target for therapeutic intervention.

Neoplasia (2014) 16, 757–769

Introduction

Thyroid cancer is the most common malignancy of the endocrine organs. The follicular cell–derived cancers are classified into well-differentiated papillary and follicular carcinomas, poorly differentiated carcinoma, and undifferentiated carcinoma. Undifferentiated thyroid carcinoma is one of the most aggressive malignancies. It spreads quickly to other organs and does not respond well to radioiodine therapy. So far, no effective target treatments are available. Ten-year survival rate is less than 10% [1].

Among prevalent genetic alterations found in undifferentiated thyroid cancer are point mutations of the *RAS*, *TP53*, and *CTNNB1* genes. Pathway analysis shows that these mutations lead to activated mitogen-activated protein kinases (MAPK) and phosphatidylinositol 3-kinase (PI3K)–protein kinase B (AKT) signaling pathways critical for the development of thyroid cancer. While mutations in the *TP53* and *CTNNB1* genes are found only in undifferentiated thyroid cancers [1], mutations in the *RAS* gene are frequently found in well-differentiated thyroid cancer. These RAS mutations could represent an early event in thyroid carcinogenesis. It is unclear, however, how *RAS* mutations could initiate undifferentiated thyroid carcinoma, especially in view of the findings that the *Ras* mutations alone in the thyroid failed to induce thyroid cancer in mice [2,3].

Previously, we demonstrated that mice with a mutant thyroid hormone receptor β, TRβPV ($Thrb^{PV/PV}$), spontaneously develop

Address all correspondence to: Dr. Sheue-yann Cheng, Laboratory of Molecular Biology, National Cancer Institute, 37 Convent Dr, Room 5128, Bethesda, MD 20892-4264, US.
E-mail: chengs@mail.nih.gov

[1] This research was supported by the Intramural Research Program of the Center for Cancer Research, National Cancer Institute, National Institutes of Health. Disclosure of potential conflicts of interest: The authors declare no conflicts of interest.
[2] This article refers to supplementary materials, which are designated by Figures S1 and S2 and are available online at www.neoplasia.com.
Received 17 June 2014; Revised 8 August 2014; Accepted 12 August 2014

1476-5586/14
http://dx.doi.org/10.1016/j.neo.2014.08.003

well-differentiated follicular thyroid cancer with similar pathologic progression and frequency of metastasis as in human thyroid cancer [4,5]. The PV mutation was originally identified in a patient with resistance to thyroid hormone [6]. The PV mutation has completely lost T3 binding activity and transcription capacity. It acts to abnormally regulate the expression of the T3 target gene through dominant negative activity. Detailed pathway analysis in the thyroid tumors of $Thrb^{PV/PV}$ mice indicated that the PI3K-AKT signaling pathway, which is frequently activated in undifferentiated thyroid carcinoma [7], is aberrantly overactivated in $Thrb^{PV/PV}$ mice [8]. CTNNB1 signaling is also increased in these mice [9,10], which was proposed to initiate tumor dedifferentiation in the late stage of tumorigenesis [1]. However, the RAS mutant–activated MAPK pathway, critical for undifferentiated thyroid carcinoma, is apparently not altered in the thyroid of $Thrb^{PV/PV}$ mice. We hypothesized that activation of the MAPK pathway driven by RAS mutation in the thyroid of $Thrb^{PV/PV}$ mice might phenotypically mimic the altered signaling observed in human thyroid cancer, thereby initiating undifferentiated thyroid cancer.

To investigate this question, we genetically introduced the $Kras^{G12D}$ mutation to express specifically in the thyroids of the $Thrb^{PV/PV}$ mice. Our aim was to learn whether the mice with *ThrbPV* and $Kras^{G12D}$ double mutations would begin developing undifferentiated thyroid carcinoma. Indeed, we found the occurrence of anaplastic foci with a high frequency in the thyroid of $Thrb^{PV/PV}Kras^{G12D}$ mice. These anaplastic foci had lost normal thyroid follicular morphology and the expression of transcription factor paired box gene 8 (PAX8). We demonstrated that synergistic signaling of TRβPV and $KRAS^{G12D}$ mutants led to an elevated level of MYC protein to suppress the *Pax8* expression through a *Pax8* upstream enhancer. Thus, our study established a mouse model of undifferentiated thyroid cancer that could further be used to understand altered signaling pathways of undifferentiated thyroid cancer.

Materials and Methods

Experimental Animals

All animal experiments were performed according to the protocols approved by the Animal Care and Use Committee at the National Cancer Institute. The $Thrb^{PV/+}$, $Kras^{LSL\text{-}G12D/+}$, *TPO-Cre (Cre)* mice were previously described [4,11,12]. Mice were in a mixed C57BL/6 and 129Svj genetic background. Thyroids and other tissues were harvested from the mice and wild-type (WT) littermates for weighing, histologic analysis, and biochemical studies.

Generation of Rat pccl3 Cell Lines Stably Expressing TRβ, TRβPV, or MYC

Rat thyroid pccl3 cells were cultured in Ham's F-12 medium supplemented with 10% FBS and containing six hormones (1 mU/ml bovine thyroid stimulating hormone (TSH), 10 μg/ml insulin, 5 μg/ml transferrin, 10 ng/ml glycyl-L-histidyl-L-lysine, 10 ng/ml somatostatin, and 0.36 ng/ml hydrocortisone; 6H medium). The pccl3 cells were transfected with an expression plasmid containing cDNA encoding *THRB*, *THRBPV*, *MYC*, or the control empty vectors and selected with G418, puromycin (Invitrogen, Carlsbad, CA), or blasticidin for 2 weeks. The expression of TRβ, TRβPV, or MYC protein was verified by Western blot analysis using monoclonal anti-TRβ/anti-TRβPV antibody (J53) or anti-MYC antibody.

Adenovirus Infection of Rat pccl3 Cells Expressing TRβ, TRβPV, or $KRAS^{G12D}$

Rat thyroid pccl3 cells were cultured in Ham's F-12 medium supplemented with 10% FBS and containing six hormones. Before addition of adenovirus, the cells were cultured in Opti-MEM I medium (Life Science, Grand Island, NY). The pccl3 cells were infected with adenovirus at a 5:1 ratio of adenovirus to pccl3 cells. After 5 hours, the medium was changed to Ham's F-12 medium supplemented with 10% thyroid hormone deficient serum (Td) and containing six hormones in the absence or presence of 100 nM T3. After 18 hours, the cells were collected for the preparation of total RNA or to prepare cell lysates for Western blot analysis.

Western Blot Analysis

The Western blot analysis was carried out as described by Furumoto et al. [13]. Primary antibodies for phosphorylated extracellular signal regulated kinase (ERK) (p-ERK; #4376S), total ERK (#9102), and glyceraldehyde-3-phosphate dehydrogenase (GAPDH; #2118) were purchased from Cell Signaling Technology (Danvers, MA). anti-TTF1 (sc-13040) antibody was purchased from Santa Cruz Biotechnology (Santa Cruz, CA). anti-PAX8 antibody (10336-1-AP) was purchased from Proteintech Group, Inc. (Chicago, IL). Cyclin D1 (RB-9041-P0) was purchased from Neomarkers (Fremont, CA). Antibodies were used at a concentration recommended by the manufacturers. For control of protein loading, the blot was probed with the antibody against GAPDH.

Electrophoretic Mobility Gel Shift Assays

Electrophoretic mobility gel shift assay was conducted similarly as described in [14]. Briefly, the [α-32P]-dCTP–labeled probes were incubated with the *in vitro* synthesized TRβ1, TRβ1PV, RXRβ, or MYC and the reaction mixture was analyzed by 5% polyacrylamide gel electrophoresis. The gel was dried and autoradiographed.

Histologic Analysis and Immunohistochemistry

Thyroid glands, heart, and lung were dissected and embedded in paraffin. Five-micrometer-thick sections were prepared and stained with hematoxylin and eosin (H&E). For each mouse, single random sections through the thyroid, lung, and heart were examined. Immunohistochemistry was performed with paraffin sections by standard methods. Dewaxed sections were treated with 0.05% citraconic anhydride buffer (pH 7.4) at 98°C for 45 minutes to expose the antigen epitopes. A primary antibody against TTF1 (sc-13040, Santa Cruz Biotechnology), PAX8 (10336-1-AP; Proteintech), or β-catenin (#9562 s; Cell Signaling Technology) was incubated with tissue section overnight at 4°C. Peroxidase activity from the secondary antibody was detected by adding substrate 3,3′-diaminobenzidine, and the sections were counterstained with hematoxylin. Bromodeoxyuridine (BrdU) incorporation assay was performed similarly as described in Zhao et al. [15].

Hormone Assays

The serum levels of total T4 (TT4) and T3 (TT3) were determined by using a Gamma Coat T4 and T3 assay RIA kit. TSH levels in serum were measured as described [15].

RNA Extraction and Real-Time Reverse Transcription–Polymerase Chain Reaction

Total RNA from thyroids was isolated using TRIzol (Invitrogen), as indicated by the protocol of the manufacturer. Real-time reverse transcription–polymerase chain reaction (RT-PCR) was performed

using a QuantiTect SYBR green RT-PCR kit from Qiagen (Valencia, CA), following the instructions of the manufacturer. Primers were as follows: for mouse *Pax8*, forward, 5′-caccctcaatgcctttcc-3′; reverse, 5′-aatacggggtgtggctgtag-3′; for the endogenous control gene mouse *Gapdh*, forward, 5′-cgtcccgtagacaaaatggt-3′; reverse, 5′-gaatttgccgt gagtggagt-3′.

Luciferase Reporter Assay

The *Pax8* upstream enhancer element cloned into pGL3b (CNS87-pGL3b) was generously provided by Dr R. Di Lauro [16]. Established rat thyroid pccl3 cells stably expressing TRβ, TRβPV, or MYC were seeded at a density of 5×10^5 in six-well culture plates and preincubated for 24 hours with Td medium. Cells were transfected using Lipofectamine 2000 (Invitrogen). Cells were lysed 24 hours later with 1 × cell lysis buffer (Promega, Madison, WI), and luciferase activity was measured using Victor 3 (PerkinElmer Life and Analytical Sciences, Waltham, MA). Luciferase values were standardized to the ratio of β-galactosidase activity and protein concentration.

Statistical Analysis

All data are expressed as means ± standard errors. Statistical analysis was performed and $P < .05$ was considered significant. All statistical tests were two-sided. GraphPad Prism version 5.0 for Mac OS X was used to perform Kaplan-Meier cumulative survival analysis, Student's *t* test, Chi-square test, and analysis of variances (ANOVAs).

Results

$Thrb^{PV/PV}Kras^{G12D}$ Mice Manifest Poor Survival with Markedly Enlarged Thyroids

To investigate whether $Thrb^{PV/PV}Kras^{G12D}$ mice develop undifferentiated thyroid cancer, we targeted the $Kras^{G12D}$ mutation to the thyroid epithelial cells of $Thrb^{PV/PV}$ mice through *TPO-Cre*–mediated expression of the $Kras^{G12D}$ gene after removal of the STOP cassette. We crossed three lines of $Thrb^{PV/+}$, $Kras^{LSL\text{-}G12D/+}$, and *TPO-Cre* mice to generate the mice with four different genotypes: $Thrb^{+/+}Kras^{+/+}Cre^{-}$, $Thrb^{+/+}Kras^{LSL\text{-}G12D/+}Cre^{+}$, $Thrb^{PV/PV}Kras^{+/+}Cre^{-}$, and $Thrb^{PV/PV}Kras^{LSL\text{-}G12D/+}Cre^{+}$, and we designate them in the following description as WT, $Kras^{G12D}$, $Thrb^{PV/PV}$, and $Thrb^{PV/PV}Kras^{G12D}$ mice, respectively.

To examine whether the expression of the $Kras^{G12D}$ and the *Cre* genes in the thyroids of $Thrb^{PV/PV}Kras^{G12D}$ mice led to functional activation of the MAPK signaling, we evaluated the phosphorylation status of the downstream effector, ERK. p-ERK, a signature of downstream Ras signaling, was assessed by Western blot analysis (Figure 1*A*, *I-a*). GAPDH was used as the loading control (Figure 1*A*, *I-e*). The protein levels of p-ERK were increased by ~ 5- and 14-fold in $Kras^{G12D}$ and $Thrb^{PV/PV}Kras^{G12D}$ mice, respectively (compare lanes 3 and 4 with 1 and 2, and lanes 7 and 8 with 5 and 6; Figure 1*A*, *I-a*), indicating that the $Kras^{G12D}$ mutant was functionally expressed in the thyroids of $Thrb^{PV/PV}Kras^{G12D}$ mice. There was also a higher p-ERK activation in $Thrb^{PV/PV}Kras^{G12D}$ mice than in $Kras^{G12D}$ mice (compare lanes 7 and 8 with lanes 3 and 4). In addition, we also found that AKT was more activated in thyroid tumors of $Thrb^{PV/PV}Kras^{G12D}$ mice (lanes 7 and 8) than in $Thrb^{PV/PV}$ mice (lanes 5 and 6) and $Kras^{G12D}$ mice (lanes 3 and 4; Figure 1*A*, I-c and I-d). Quantitative analysis of p-ERK, total ERK, p-AKT, and total AKT band intensities indicated that the p-ERK/total ERK ratio and p-AKT/total AKT was 1.5-fold and 1.9-fold higher in $Thrb^{PV/PV}Kras^{G12D}$ mice than in $Kras^{G12D}$ mice, respectively (Figure 1*A*, *II* and *III*). Previously, we have shown that AKT was activated in thyroid tumors of $Thrb^{PV/PV}$ mice [8]. These results suggest the contribution of TRβPV in the further activating of $KRAS^{G12D}$ and AKT signaling.

Analysis of Kaplan-Meier cumulative survival curves was conducted for WT, $Kras^{G12D}$, $Thrb^{PV/PV}$, and $Thrb^{PV/PV}Kras^{G12D}$ mice over a period of 10.5 months (Figure 1*B*). No WT mice or $Kras^{G12D}$ mice died during that period, but about 30% of $Thrb^{PV/PV}$ mice died. By contrast, only 50% of $Thrb^{PV/PV}Kras^{G12D}$ mice lived to the age of 4.8 months, and none survived beyond 10.5 months. The differences between the survival rates of the $Thrb^{PV/PV}$ and $Thrb^{PV/PV}Kras^{G12D}$ mice were highly significant ($P < .01$). These results indicate that synergistic effects of TRβPV and $KRAS^{G12D}$ mutants led to poor survival of $Thrb^{PV/PV}Kras^{G12D}$ mice.

The thyroid weights of $Kras^{G12D}$ mice (3.6 ± 0.6 mg, $n = 13$) were similar to those of WT mice (2.7 ± 0.3 mg, $n = 13$; Figure 1*C*, bar 2 *vs* 1). This observation is consistent with a previous report that $Kras^{G12D}$ mutation alone is not sufficient to increase the thyroid weight [2]. The thyroid of $Thrb^{PV/PV}$ mice was markedly enlarged with an average weight of 84 mg (84.47 ± 11.11 mg, $n = 29$). Among mice with four genotypes, the double mutant mice had the largest thyroid (216.7 ± 18.52 mg, $n = 54$). The increase in thyroid weight of $Thrb^{PV/PV}Kras^{G12D}$ mice was 80-, 60-, and 2.6-fold greater than in WT, $Kras^{G12D}$, and $Thrb^{PV/PV}$ mice, respectively (bar 4 *vs* 1, bar 4 *vs* 2, bar 4 *vs* 3; Figure 1*C*).

Increased Thyroid Growth in $Thrb^{PV/PV}Kras^{G12D}$ Mice Is Not Mediated by Elevated TSH Levels

TSH is the major stimulator of thyrocyte proliferation, and its levels are regulated by the thyroid hormones (T4 and T3) through a negative feedback loop [17]. To evaluate whether TSH could contribute to the markedly increased thyroid growth in $Thrb^{PV/PV}Kras^{G12D}$ mice, we compared serum TSH, serum total T4, and total T3 between $Thrb^{PV/PV}$ and $Thrb^{PV/PV}Kras^{G12D}$ mice (Figure 2). There were no significant differences between $Thrb^{PV/PV}$ and $Thrb^{PV/PV}Kras^{G12D}$ mice in serum levels of TSH (WT: 38.3 ± 7.4 ng/ml, $n = 18$; $Kras^{G12D}$: 14.8 ± 4.2 ng/ml, $n = 10$; $Thrb^{PV/PV}$: 28420 ± 6969 ng/ml, $N = 9$; $Thrb^{PV/PV}Kras^{G12D}$: 39990 ± 5331 ng/ml, $n = 11$; Figure 2*A*), total T4 (WT: 2.6 ± 0.2 μg/ml, $n = 10$; $Kras^{G12D}$: 4.0 ± 0.5 μg/ml, $n = 9$; $Thrb^{PV/PV}$: 27.7 ± 1.3 μg/ml, $n = 14$; $Thrb^{PV/PV}Kras^{G12D}$: 19.6 ± 2.7 μg/ml, $n = 9$; Figure 2*B*), and total T3 (WT: 1.0 ± 0.1 ng/ml, $N = 6$; $Kras^{G12D}$: 1.0 ± 0.2 ng/ml, $n = 9$; $Thrb^{PV/PV}$: 7.2 ± 0.7 ng/ml, $n = 9$; $Thrb^{PV/PV}Kras^{G12D}$: 4.9 ± 0.9 ng/ml, $n = 10$; Figure 2*C*). These data indicated that $Kras^{G12D}$ activation in thyroids did not further affect the hypothalamus-pituitary-thyroid axis in $Thrb^{PV/PV}Kras^{G12D}$ mice. Thus, the increased thyroid weight in $Thrb^{PV/PV}Kras^{G12D}$ mice was not due to an elevated TSH level (Figure 2*A*).

Increased Proliferation of Thyroid Tumor Cells in $Thrb^{PV/PV}Kras^{G12D}$ Mice

To determine whether the increased thyroid growth was due to increased proliferation of tumor cells in $Thrb^{PV/PV}Kras^{G12D}$ mice, we examined BrdU incorporation in the thyroids of mice with four genotypes (Figure 3*A*). As a positive control, we also examined BrdU incorporation in the intestines. Intensively stained cells were seen in the intestines (Figure 3, *A-e* and *A-f*). In contrast, no nuclei with BrdU-positive cells were observed in the thyroid sections of WT mice (Figure 3*A-a*), and only a few were detected in the thyroid sections of $Kras^{G12D}$ mice (Figure 3*A-b*). However, nuclei with BrdU incorporation were clearly detected in thyroid sections of $Thrb^{PV/PV}$ mice (Figure 3*A-c*) and $Thrb^{PV/PV}Kras^{G12D}$ mice (Figure 3*A-d*), with significantly more in the $Thrb^{PV/PV}Kras^{G12D}$ than the $Thrb^{PV/PV}$

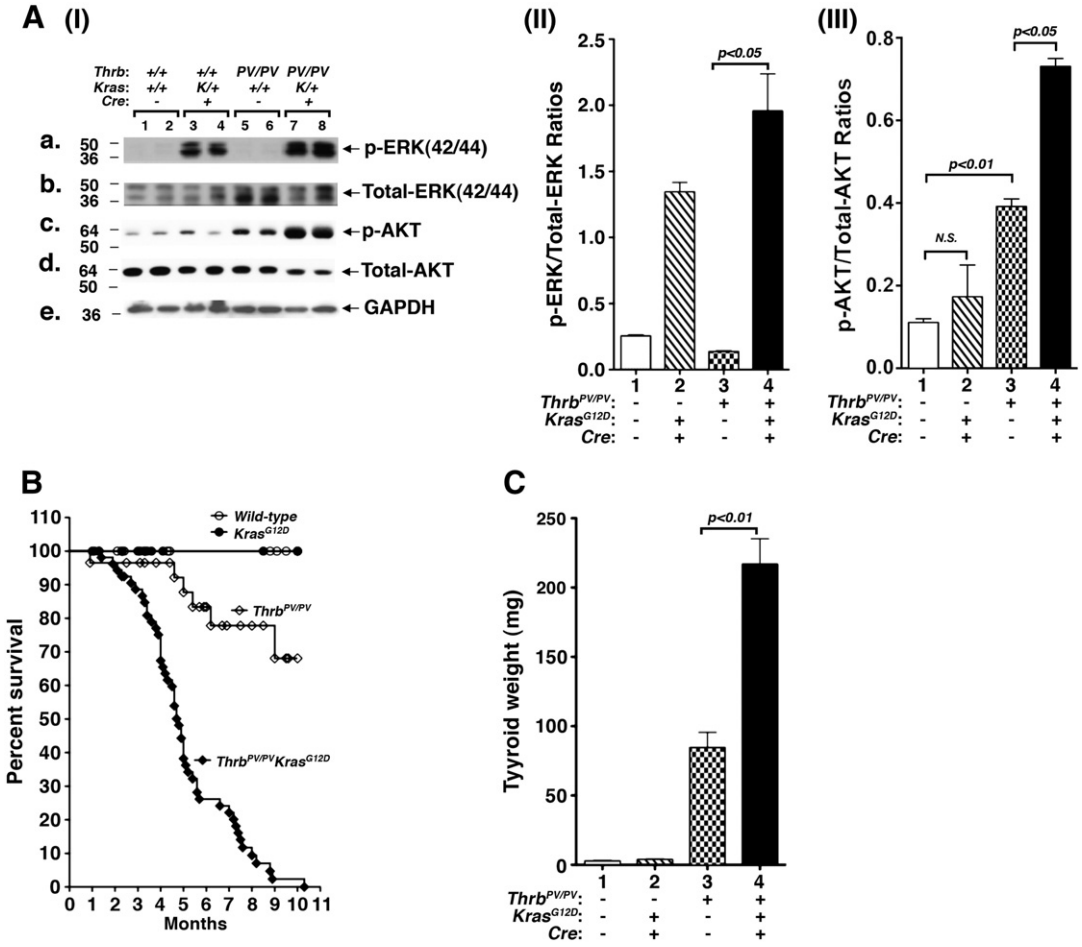

Figure 1. Poor survival of *Thrb*$^{PV/PV}$*Kras*^{G12D} mice. (A-I) Protein levels of ERK and AKT in the thyroids of WT, *Kras*^{G12D}, *Thrb*$^{PV/PV}$, and *Thrb*$^{PV/PV}$*Kras*^{G12D} mice. Western blot analyses for p-ERK (a), total ERK (b), phosphorylated AKT (c), total AKT (d), and GAPDH (e), as loading control, were carried out as described in the Materials and Methods section. Representative results from two mice are shown and the genotypes are marked. (A-II) The band intensities were quantified by image analysis and p-ERK/total ERK ratios were determined using GAPDH as loading control. (A-III) The band intensities were quantified by image analysis and p-AKT/total AKT ratios were determined using GAPDH as loading control. (B) The Kaplan-Meier survival curves for WT, *Kras*^{G12D}, *Thrb*$^{PV/PV}$, and *Thrb*$^{PV/PV}$*Kras*^{G12D} mice up to 10.5 months of age. The Kaplan-Meier cumulative survival analysis was performed using GraphPad Prism version 5.0 for Mac OS X. Survival rates of *Thrb*$^{PV/PV}$*Kras*^{G12D} (n = 42) and mice with other genotypes were significantly different (P < .01). (C) Thyroid glands of the mice with four genotypes (n = 9-22) were dissected and compared in the same age groups. The difference in the thyroid weight between *Thrb*$^{PV/PV}$*Kras*^{G12D} mice and the mice with other genotypes was significant at 2 to 10.4 months (P < .01), as determined by ANOVA.

mice (compare Figure 3*A-d* to Figure 3*A-c*). To quantify the percentage of cells undergoing active cell cycling within a 2-hour BrdU-labeling period, we calculated the average ratios of BrdU-positive cells to total cells from 10 to 12 bright fields at high magnification (×400) of each section. The quantitative data are shown in Figure 3*B*. In WT mice, no BrdU-positive stained cells were observed (bar 1, Figure 3*B*). In *Kras*^{G12D} mice, less than 1% of cells were BrdU-positive (bar 2, Figure 3*B*). However, 3.8% of cells from *Thrb*$^{PV/PV}$ mice were actively proliferating (bar 3, Figure 3*B*). In *Thrb*$^{PV/PV}$*Kras*^{G12D} mice, the ratio increased to 9.3% (bar 4, Figure 3*B*), indicating a 2.4-fold increase in the proliferation of thyroid tumor cells of *Thrb*$^{PV/PV}$*Kras*^{G12D} mice. These findings indicated that enhanced proliferation contributed to the marked thyroid enlargement of *Thrb*$^{PV/PV}$*Kras*^{G12D} mice.

Thrb$^{PV/PV}$*Kras*^{G12D} *Mice Develop Anaplastic Foci with High Frequency*

We performed histopathologic analysis to determine whether *Thrb*$^{PV/PV}$*Kras*^{G12D} mice developed undifferentiated thyroid cancer (Figure 4*A*). Thyroids of *Kras*^{G12D} mice exhibited no apparent abnormalities. As we previously observed, thyroid of the *Thrb*$^{PV/PV}$ mouse displayed extensive hyperplasia at an early stage (data not shown). In the thyroid of *Thrb*$^{PV/PV}$*Kras*^{G12D} mice, aggressive phenotypes were apparent at the age of 1 to 2 months. Hyperplasia (Figure 4*A-a*), advanced capsular invasion (Figure 4*A-b*), and vascular invasion (Figure 4*A-b*) were frequently observed at a younger age of 2 to 5 months. Moreover, lung metastases (Figure 4*A-e*) were frequently observed in *Thrb*$^{PV/PV}$*Kras*^{G12D} mice at the same age. The metastases in the heart were also observed in *Thrb*$^{PV/PV}$*Kras*^{G12D} mice (Figure 4*A-f*). Importantly, we identified many anaplastic foci (Figure 4*A-c*, indicated by arrows) at the young age of 2 to 5 months under low magnification. Under high magnification (×400; Figure 4*A-d*, indicated by arrow), it was clear that the anaplastic foci completely lost the normal morphology of thyroid follicular cells. These observations indicated that *Thrb*$^{PV/PV}$*Kras*^{G12D} mice developed undifferentiated thyroid cancer.

The detailed pathohistologic analyses are summarized in Figure 4*B*. From 2 to 5 months of age, all *Thrb*$^{PV/PV}$ mice and *Thrb*$^{PV/PV}$*Kras*^{G12D}

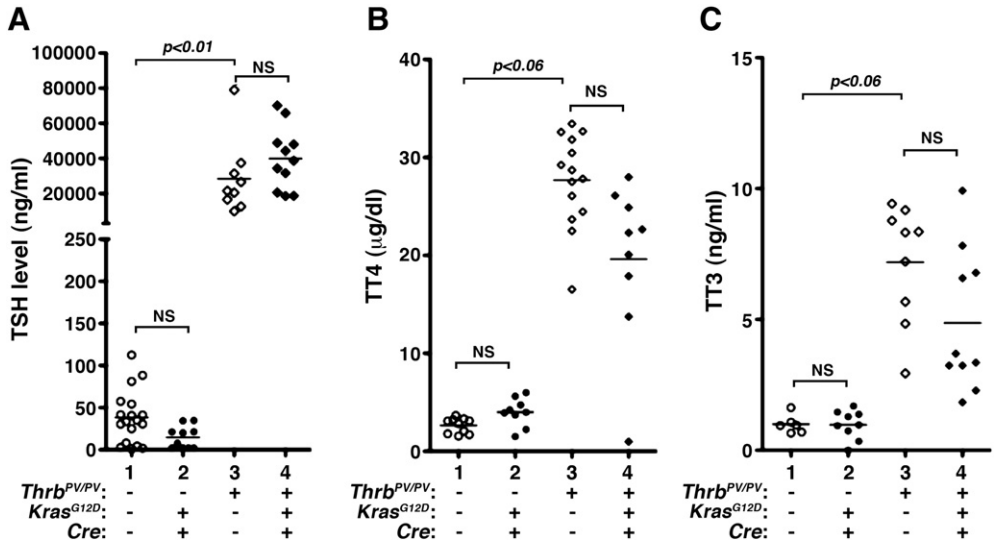

Figure 2. No significant differences in thyroid function tests between *Thrb*$^{PV/PV}$ and *Thrb*$^{PV/PV}$*Kras*^{G12D} mice. Serum total TSH (A), total T4 (TT4, B), and total T3 (TT3, C) of WT, *Kras*^{G12D}, *Thrb*$^{PV/PV}$, and *Thrb*$^{PV/PV}$*Kras*^{G12D} mice were determined as described in the Materials and Methods section. The *P* values are marked (n = 5-14).

mice displayed thyroid hyperplasia. The occurrence of capsular invasion in the thyroid was found in 94% of the *Thrb*$^{PV/PV}$*Kras*^{G12D} mice but only 25% of the *Thrb*$^{PV/PV}$ mice at the same age (Figure 4*B-a*). Vascular invasion developed in the thyroids of 4% of *Thrb*$^{PV/PV}$ mice and 75% of *Thrb*$^{PV/PV}$*Kras*^{G12D} mice (Figure 4*B-b*). It was noted that thyroid anaplasia, which was not observed before 5 months of age in *Thrb*$^{PV/PV}$ mice, occurred at the young age of 2 to 5 months in *Thrb*$^{PV/PV}$*Kras*^{G12D} mice. At age of 2 to 5 months, 63% of *Thrb*$^{PV/PV}$*Kras*^{G12D} mice

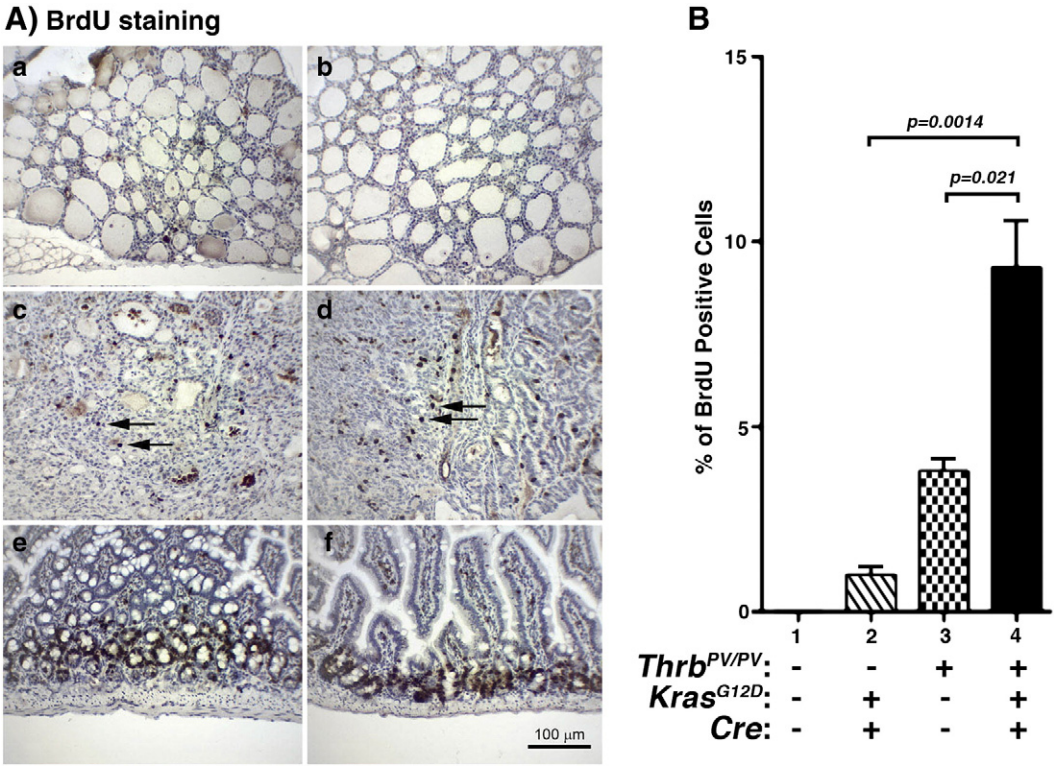

Figure 3. Proliferation of thyroid tumor cells is increased in *Thrb*$^{PV/PV}$*Kras*^{G12D} mice. (A) Thyrocyte proliferation in WT (a), *Kras*^{G12D} (b), *Thrb*$^{PV/PV}$ (c), and *Thrb*$^{PV/PV}$*Kras*^{G12D} (d) mice was revealed by BrdU incorporation assay as described in the Materials and Methods section. A representative image of BrdU-positive thyrocytes (indicated by arrows) in different groups of mice is shown at × 400 magnification. Small intestine tissues of WT (e) and *Kras*^{G12D} (f) mice were used as positive controls of highly proliferative tissues. (B) Quantification of BrdU-positive cells in thyroid sections of WT, *Kras*^{G12D}, *Thrb*$^{PV/PV}$, and *Thrb*$^{PV/PV}$*Kras*^{G12D} mice. The percentage of BrdU-positive cells *versus* total cells was determined from 10 to 12 bright fields, as shown in A.

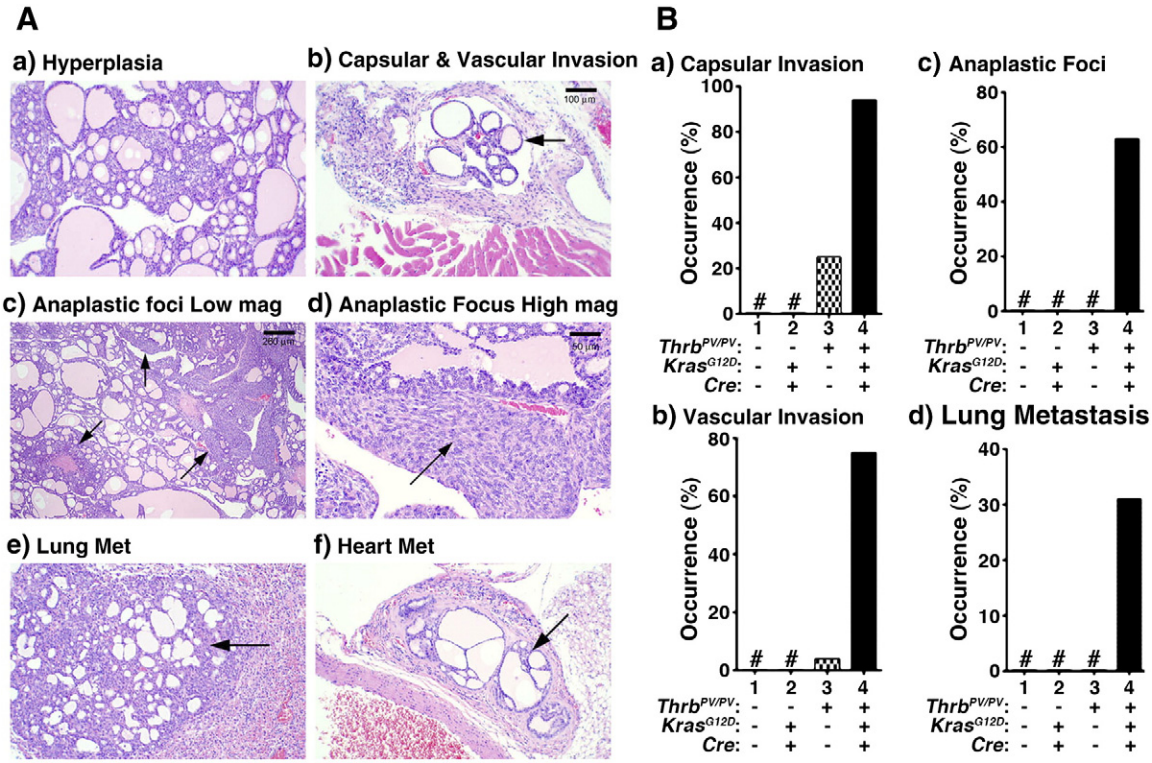

Figure 4. Histopathologic features of thyroid carcinoma of *Thrb*$^{PV/PV}$*Kras*^{G12D} mice. (A) H&E staining of thyroids, lung, or heart from the *Thrb*$^{PV/PV}$*Kras*^{G12D} mice. Panels show (a) hyperplasia, (b, arrow) capsular invasion and vascular invasion, (c and d, arrows), anaplastic foci, (e, arrow), microscopic lung metastases, and (f, arrow) heart metastases in *Thrb*$^{PV/PV}$*Kras*^{G12D} mice at 2 to 5 months of age. (B) Quantitative analysis of occurrence frequency (%) of (a) capsular invasion, (b) vascular invasion, (c) anaplastic foci, and (d) lung metastasis of WT, *Kras*^{G12D}, *Thrb*$^{PV/PV}$, and *Thrb*$^{PV/PV}$*Kras*^{G12D} mice. Sections of thyroids and lungs were stained with H&E and analyzed for pathologic progression. The data are expressed as the percentage of occurrence frequency of the mice examined. The designation (#) indicates zero occurrence frequency (%).

developed anaplasia, whereas no *Thrb*$^{PV/PV}$ mice did (Figure 4*B-c*). Metastasis in the lung occurred in 31% of *Thrb*$^{PV/PV}$*Kras*^{G12D} mice at age of 2 to 5 months, but no metastasis was detected in *Thrb*$^{PV/PV}$ mice at the same age (Figure 4*B-d*). Interestingly, metastasis in the heart was also observed in *Thrb*$^{PV/PV}$*Kras*^{G12D} mice (6%; Figure 4*A-f*). These results show that while *Thrb*$^{PV/PV}$ mice developed differentiated thyroid cancer, *Thrb*$^{PV/PV}$*Kras*^{G12D} mice developed aggressive anaplastic thyroid carcinomas.

Decreased Expression of the Transcription Factor PAX8 and TTF1 Genes in Thyroid Anaplastic Foci in Thrb$^{PV/PV}$*Kras*^{G12D} *mice*

Thyroid-specific transcription factors, PAX8 and TTF1, are essential for thyroid organogenesis and differentiation. It is known that decreased PAX8 nuclear abundance was detected in anaplastic carcinomas [18] and that TTF1 is often lost in anaplastic thyroid cancer [19]. We therefore analyzed the expression of the PAX8 and TTF1 protein levels by Western blot assays. In all thyroid tumors of *Thrb*$^{PV/PV}$ mice, we detected abundant PAX8 and TTF1 proteins (panels *a* and *b*, lanes 5 and 6; Figure 5, *A* and *B*), which were significantly higher than those in WT or *Kras*^{G12D} mice (panels *a* and *b*, lanes 1-4; Figure 5, *A* and *B*). However, we detected two major expression patterns of PAX8 and TTF1 proteins in thyroid tumors of *Thrb*$^{PV/PV}$*Kras*^{G12D} mice (Figure 5, *A* and *B*). One prominent pattern was the reduced abundance of PAX8 and TTF1 proteins (lanes 7-9, Figure 5*A*) that was clearly lower than that in WT mice (lanes 1 and 2), *Kras*^{G12D} mice (lanes 3 and 4), and *Thrb*$^{PV/PV}$ mice (lanes 5 and 6). However, in some thyroid tumors, the abundance of PAX8 and TTF1 proteins was at a similar level as that in *Thrb*$^{PV/PV}$ mice (Figure 5*B*, lanes 7 and 8 *vs* lanes 5 and 6).

The findings that these two thyroid differentiation markers displayed two different patterns prompted us to use immunohistochemical analysis to probe further their distribution and abundance in thyroid tumor cells. The nuclear staining of PAX8 in the thyroid of WT mice was clearly evident (Figure 5*C-Ia*). Intensive staining of PAX8 was also detected in the tumor cells of *Thrb*$^{PV/PV}$ mice (Figure 5*C-Ib*), indicating that thyroid epithelial cells were well differentiated. In the thyroid tumors of *Thrb*$^{PV/PV}$*Kras*^{G12D} mice, two patterns were apparent. For well-differentiated thyroid tumors without any anaplastic foci, the stained intensity of PAX8 proteins was similar to tumor cells observed in *Thrb*$^{PV/PV}$ mice. For the undifferentiated tumors with anaplastic foci, there was only background staining for the PAX8 proteins, indicating the loss of PAX8 expression as outlined by dots (Figure 5*C-Ic*). Similarly, intensive TTF1 nuclear staining was detected in the thyroid of WT mice (Figure 5*C-IIa*) and in the tumor cells of *Thrb*$^{PV/PV}$ mice (Figure 5*C-IIb*). In contrast, it was clear that staining of the nuclear TTF1 in the anaplastic foci was markedly reduced (Figure 5*C-IIc*). These results suggest that consistent with findings in human anaplastic thyroid cancer [19], the loss of PAX8 and TTF1 expression was associated with loss of differentiation of thyroid follicular cells and that the expression of PAX8 or TTF1 was related to the differentiation status of thyroid tumors.

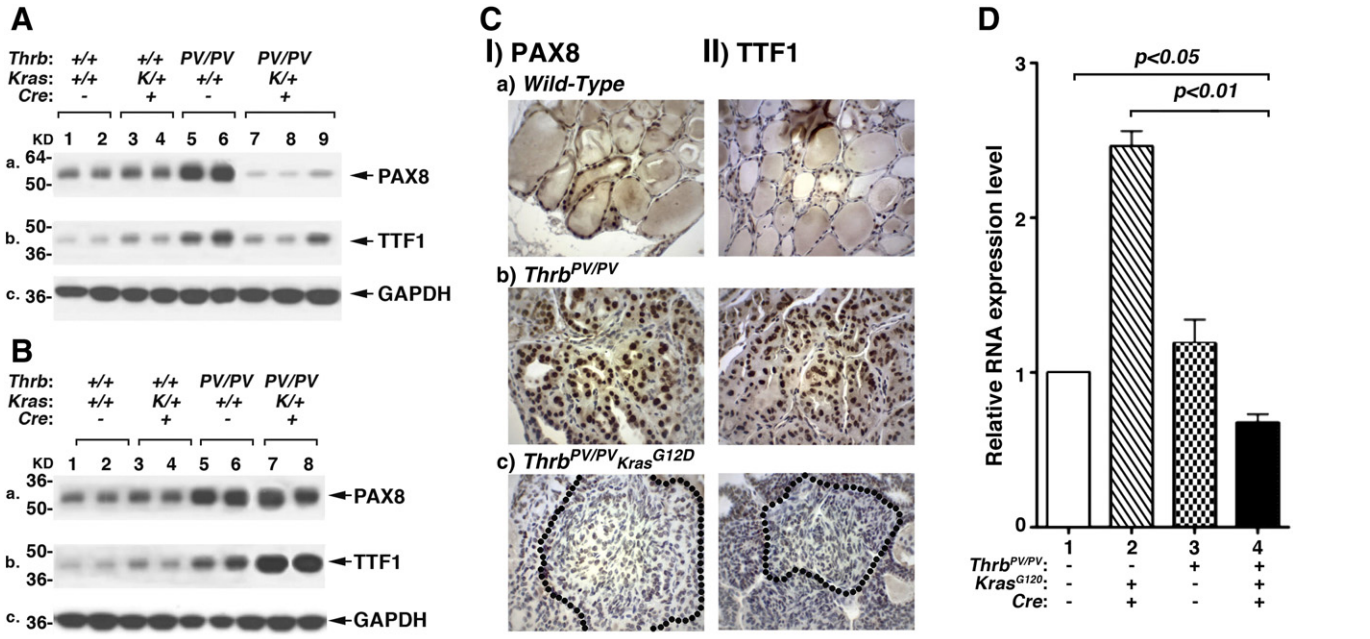

Figure 5. Decreased expression of transcription factor PAX8 within anaplastic foci in thyroid carcinomas of $Thrb^{PV/PV}Kras^{G12D}$ mice. (A and B) Protein level of PAX8 (a) and TTF1 (b) and loading control GAPDH (c) in WT, $Kras^{G12D}$, $Thrb^{PV/PV}$, and $Thrb^{PV/PV}Kras^{G12D}$ thyroids as marked. Total protein extracts were prepared from thyroids of WT and $Kras^{G12D}$ mice and thyroid tumors of $Thrb^{PV/PV}$ and $Thrb^{PV/PV}Kras^{G12D}$ mice aged 2 to 5 months. (C) Immunohistochemical analysis of protein abundance of the PAX8 (I) and TTF1 (II) in thyroids. Sections of thyroids derived from WT (a), $Thrb^{PV/PV}$ (b), and $Thrb^{PV/PV}Kras^{G12D}$ (c) mice were treated with anti-PAX8 or TTF1 antibodies as described in the Materials and Methods section. The anaplastic foci in the thyroid tumors are outlined by dots. (D) The mRNA level of the *Pax8* gene was measured by real-time RT-PCR. Reactions were performed in 50 ng of total RNA from five mouse thyroid samples from each group. *Gapdh* gene was used as a reference. A lower level of *Pax8* mRNA was detected in $Thrb^{PV/PV}Kras^{G12D}$ mice than in WT mice.

We further examined the *Pax8* mRNA expression in the thyroid tumors with anaplastic foci. As shown in Figure 5*D*, *Pax8* mRNA expression was lower (35% reduction, $n = 12$) in $Thrb^{PV/PV}Kras^{G12D}$ mice (bar 4, Figure 5*D*) than in WT mice (bar 1). The decreased *Pax8* mRNA expression suggested that the PAX8 was likely, at least in part, the effector/regulator of undifferentiation in thyroid carcinoma.

MYC and PAX8 Protein Levels Are Inversely Correlated in Thyroid Tumors of $Thrb^{PV/PV}Kras^{G12D}$ Mice

To dissect the molecular events responsible for promoting dedifferentiation in the thyroid tumors of $Thrb^{PV/PV}Kras^{G12D}$ mice, we screened for altered expression in regulators known to be involved in the dedifferentiation process. We considered MYC because abnormal *MYC* expression is associated with dedifferentiation [20,21] and MYC is commonly elevated in anaplastic thyroid cancer [22,23]. Indeed, we found a consistent inverse correlation of MYC with PAX8 and TTF1 at the protein level in the thyroid tumors of $Thrb^{PV/PV}Kras^{G12D}$ mice. As shown in Figure 6*A*, the MYC protein level was highly elevated in thyroid tumors of $Thrb^{PV/PV}Kras^{G12D}$ mice (panel *a*, lanes 7-10, representative examples from 10 undifferentiated thyroid tumors) in which PAX8 and TTF1 protein levels were low (lanes 7-10 in panels *b* and *c*; significant correlation with Chi-square test: $P < .05$). For all thyroid tumors of $Thrb^{PV/PV}$ mice examined (representative examples, lanes 5 and 6, panel *a*, Figure 6*A*) and six thyroid tumors of $Thrb^{PV/PV}Kras^{G12D}$ mice without undifferentiated thyroid cancer, MYC protein levels were relatively low (lanes 11 and 12, panel *a*, Figure 6*A*), while TTF1 and PAX8 protein levels were higher (lanes 11 and 12, panels *b* and *c*; significant correlation with Chi-square test: $P < .05$). Very low MYC protein abundance was observed in WT mice (lanes 1 and 2, Figure 6*A-a*) and $Kras^{G12D}$ mice (lanes 3 and 4, Figure 6*A-a*), while TTF1 and PAX8 protein levels were high (lanes 1-4, Figure 6*A*, panels *b* and *c*). The band intensities in Figure 6*A* were quantified, and Figure 6*B* shows the quantitative data for MYC (panel *a*), TTF1 (panel *b*), and PAX8 (panel *c*) with different phenotypes. Consistent with the reports that MYC is commonly elevated in anaplastic thyroid cancer [22,23], these results strongly suggest that MYC is associated with the dedifferentiation process of tumor cells of $Thrb^{PV/PV}Kras^{G12D}$ mice.

We also examined the protein abundance of BIM, a proapoptotic protein, whose expression could be repressed by MYC [24,25]. Figure 6*A-d* shows that low BIM protein levels (lanes 7-10, panel *d*) were accompanied by high MYC protein levels in dedifferentiated tumor cells of $Thrb^{PV/PV}Kras^{G12D}$ mice and that high levels of BIM was associated with low MYC in differentiated tumors (lanes 11 and 12, panel *d*). The quantitative data of BIM are shown in Figure 6*B-d*. These findings indicate that lower BIM protein levels decreased apoptosis to increase tumor growth of $Thrb^{PV/PV}Kras^{G12D}$ mice.

$KRAS^{G12D}$ Collaborates with TRβPV to Increase the MYC Expression

To examine whether co-expression of $KRAS^{G12D}$ and TRβPV could upregulate MYC expression, we infected rat thyroid pccl3 cells with adenoviral vectors to express $KRAS^{G12D}$, TRβ, TRβPV, or both $KRAS^{G12D}$ and TRβPV. As shown in Figure 7*A*, neither $KRAS^{G12D}$ (bars 3 and 4), TRβ (bars 5 and 6), nor TRβPV (bars 7 and 8) alone significantly increase *Myc* mRNA expression. In fact, in the presence of T3, TRβ significantly decreased the *Myc* mRNA expression. However, co-expression of $KRAS^{G12D}$ and TRβPV led to a significant increase in

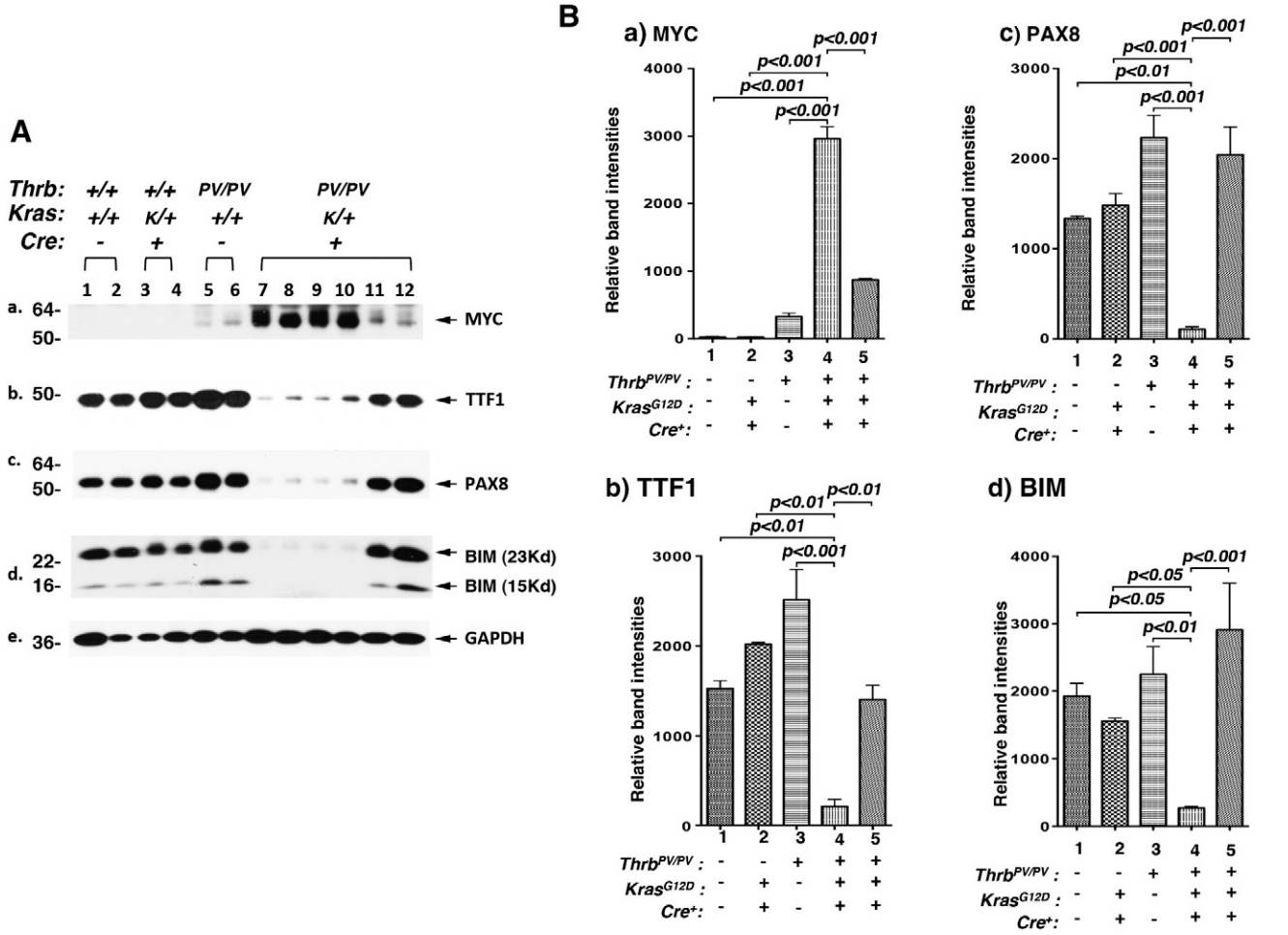

Figure 6. Inverse correlation of elevated MYC level with PAX8 and TTF1 proteins. (A) Total protein extracts were prepared from thyroids of WT ($n = 10$) and *Kras*^{G12D} ($n = 10$) mice and thyroid tumors of *Thrb*$^{PV/PV}$ ($n = 12$) and *Thrb*$^{PV/PV}$*Kras*^{G12D} ($n = 16$) mice aged 2 to 5 months. Western blot analysis was carried out for MYC (a), TTF1 (b), PAX8 (c), BIM (d), and GAPDH (e) as described in the Materials and Methods section, and the representative examples are shown. (B) The band intensities of MYC (a), TTF1 (b), PAX8 (c), and BIM (d) were quantified by image analysis and relative band intensities were determined using GAPDH as loading control. Bar 1 is from WT mice; bar 2, *Kras*^{G12D} mice; bar 3, *Thrb*$^{PV/PV}$ mice; bar 4, anaplastic thyroid tumors of *Thrb*$^{PV/PV}$*Kras*^{G12D} mice (lanes 7-10 of Figure 6*A*); and bar 5, tumors without anaplasia of *Thrb*$^{PV/PV}$*Kras*^{G12D} mice (lanes 11-12 of Figure 6*A*).

Myc mRNA expression (Figure 7*A*, bars 9 and 10). Similarly, Western blot analysis indicated that neither KRAS^{G12D}, TRβ, nor TRβPV alone increased the abundance of MYC proteins (lanes 3 and 4, 5 and 6, and 7 and 8, respectively). In the presence of T3, TRβ significantly decreased abundance of MYC. However, co-expression of KRAS^{G12D} and TRβPV significantly increased the abundance of MYC proteins (Figure 7*B*, lanes 9 and 10; Figure 7*C*, bars 9 and 10). The results indicated the T3-bound TRβ acted as a negative regulator of MYC expression and that TRβPV was no longer able to inhibit the expression of MYC as TRβ did in the presence of T3. Instead, TRβPV collaborated with KRAS^{G12D} to upregulate MYC in the pccl3 cells.

MYC Collaborates with TRβPV to Suppress the Expression of the Pax8 Gene, Increase Proliferation, and Inhibit Apoptosis

That the decreased expression of *Pax8* mRNA was associated with anaplastic foci prompted us to understand how the expression of *Pax8* was regulated in the thyroid tumors of *Thrb*$^{PV/PV}$*Kras*^{G12D} mice. Nitsch et al. identified an element in a distant upstream location of the *Pax8* gene known as lnon-coding genomic sequence (CNS) 87 (CNS87), which is responsible for the *Pax8* expression in thyroid epithelial cells [16]. We examined the CSN87 sequence and identified one potential thyroid hormone receptor response element (TRE) with two half-binding sites separated by five bases (Supplemental Figure S1-A). We designated this element as CNS-TRE. Using gel mobility shift, we found that TRβ bound to CNS-TRE as homodimers and heterodimers with the retinoid acid receptor (RXR) in a concentration-dependent manner (Supplemental Figure S1-B, lanes 4-6). The binding specificity was confirmed by antibody-induced supershift and by competition with unlabeled TRE (lanes 7 and 9, respectively). Similarly, TRβPV also bound to CNS-TRE as homodimers and as heterodimers with RXR (lanes 11-13). The binding specificity was also confirmed by antibody-induced supershift and by competition with unlabeled TRE (Supplemental Figure S1-B, lanes 14 and 16, respectively). We next mutated one base in each half-binding site to see whether binding of CNS-TRE to TRβ was specific (Supplemental Figure S1-A). As controls, both TRβ and TRβPV bound to CNS-TRE as homodimers and as heterodimers with RXR (Supplemental Figure S1-C, lanes 4 and 8). After we mutated one base in the half-binding site, neither TRβ nor TRβPV could any

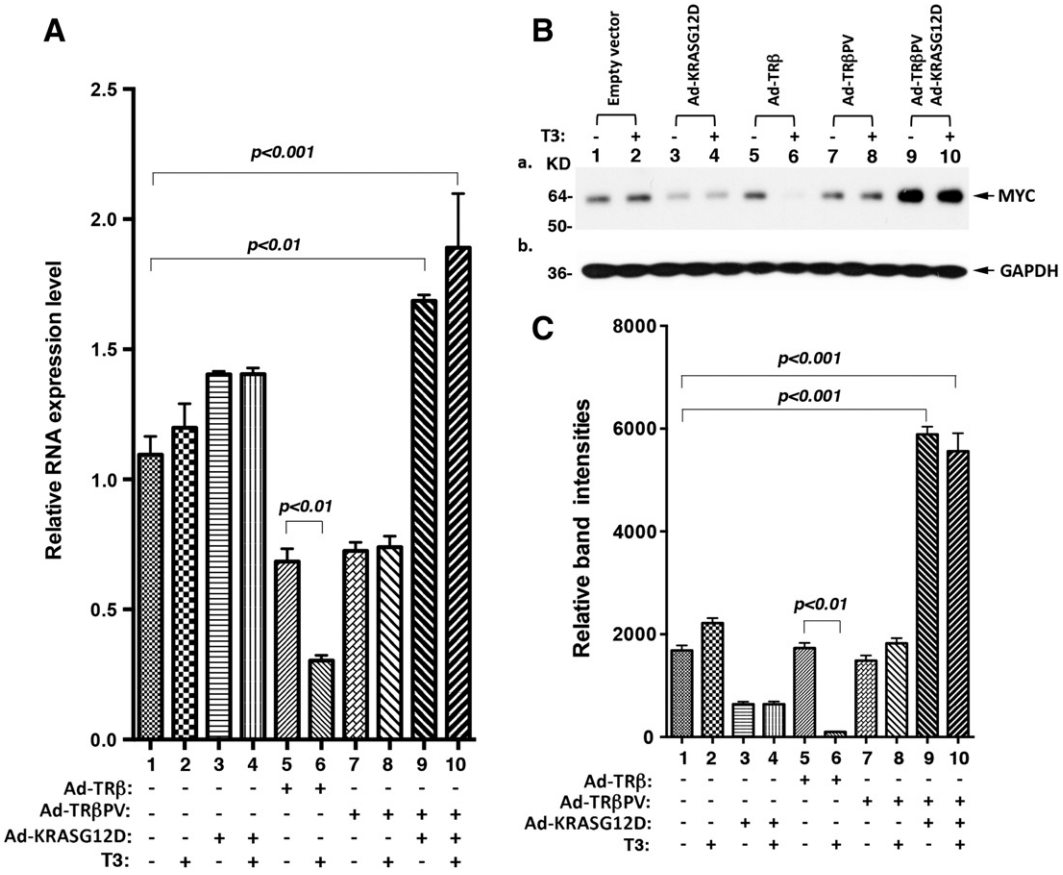

Figure 7. KRAS^{G12D} together with TRβPV increases the abundance of MYC in rat thyroid pccl3 cells. (A) The mRNA level of the *Myc* gene was measured by real-time RT-PCR in the pccl3 cells infected with control adenoviral vector or adenoviral vectors expressing KRAS^{G12D}, TRβWT, TRβPV, or both KRAS^{G12D} and TRβPV. Reactions were performed in 200 ng of total RNA from adenovirus-infected pccl3 cells. *Gapdh* gene was used as a reference. (B) Protein level of MYC in the pccl3 cells infected with control adenoviral vector or adenoviral vectors expressing KRAS^{G12D}, TRβWT, TRβPV, or both KRAS^{G12D} and TRβPV. Total protein extracts were prepared from the pccl3 cells 18 hours after adenovirus infection. (C) The band intensities were quantified by image analysis and relative band intensities were determined using GAPDH as loading control.

longer bind to mutant CNS-TRE (lanes 12-19). These mutational analyses confirmed that binding of TRβ or TRβPV to CNS-TRE was specific. Using the luciferase reporter in established rat thyroid pccl3 cells stably expressing TRβ, we examined whether TRE-containing CNS87 could mediate the T3-dependent TRβ transcriptional activity. In the presence of TRβ, luciferase activity was increased by about two-fold (Supplemental Figure S1-D). Addition of T3 further increased the luciferase activity (bar 4 *vs* bar 3). When mutated CNS-TRE was used, no reporter activity was detected (bars 5 and 6; Supplemental Figure S1-D). The results indicated that CNS87 in the *Pax8* gene was regulated by TRβ.

Comparison of the CNS87 reporter activities shows that TRβPV had lower luciferase activity than TRβ (Figure 8*A*, bar 4 *vs* bar 2). The lower luciferase activity mediated by TRβPV suggested that TRβPV could act to repress the *Pax8* expression within the anaplastic foci. Furthermore, other cellular regulator could collaborate with TRβPV to further suppress the expression of the *Pax8* gene. The strong association between the elevated MYC level and reduced PAX8 prompted us to examine whether the high MYC could collaborate with TRβPV to repress the *Pax8* expression in the thyroid tumors of *Thrb*$^{PV/PV}$*Kras*^{G12D} mice. Accordingly, we examined whether MYC affected the binding of TRβ or TRβPV to CNS-TRE. Figure 8*B-a* shows that TRβ and TRβPV bound to CNS-TRE as homodimers and heterodimers with RXR in a dose-dependent manner (lanes 3-6 and 8-11, respectively). However, in the presence of MYC, the binding intensity was reduced (Figure 8*B-a*, lanes 12-15 and 16-19, respectively). Quantitative analysis indicated that binding intensities for TRβ and TRβPV were reduced in the presence of MYC (Figure 8*B-b*), suggesting that MYC could weaken the binding of TRβ and TRβPV to CNS-TRE through direct or indirect interference. To ascertain the functional consequence of decreased binding of TRβPV binding to CNS-TRE by MYC, we carried out luciferase activities in thyroid pccl3 cells stably expressing TRβPV alone or together with MYC. Because TRβPV does not bind T3, luciferase activities in the presence of MYC were reduced in a T3-independent manner (Figure 8*C*, bars 3 and 4 *vs* bars 1 and 2). Taken together, these data suggested that MYC could collaborate with TRβPV to suppress the expression of the *Pax8* gene and induce the dedifferentiation of thyroid tumor cells.

It is known that in mammalian cells MYC not only regulates terminal differentiation but also stimulates cell proliferation and induces apoptosis [26]. Since the thyroid tumor cells of *Thrb*$^{PV/PV}$*Kras*^{G12D} mice proliferated faster than the thyroid cells of WT mice, *Kras*^{G12D} mice, and *Thrb*$^{PV/PV}$ mice (see Figures 1*C* and 3),

we also evaluated whether the upregulated MYC in thyroid tumor cells of $Thrb^{PV/PV}Kras^{G12D}$ mice (see Figure 6) led to increased expression of the key regulators of cell proliferation. Consistent with upregulated MYC shown in Figure 6, cyclin D1 was most abundantly upregulated in the thyroid tumor cells of $Thrb^{PV/PV}Kras^{G12D}$ mice (lanes 7-8; Figure 9*A-a*) as compared with WT mice (lanes 1-2), $Kras^{G12D}$ mice (lanes 3-4), and $Thrb^{PV/PV}$ mice (lanes 5-6, Figure 9*A-a*). Moreover, we also found that B-cell lymphoma 2 (BCL-2), a critical anti-apoptotic regulator, was expressed at the highest level in the thyroid tumor cells of $Thrb^{PV/PV}Kras^{G12D}$ mice (lanes 7-8, Figure 9*A-b*). Panel *c* shows the loading controls of GAPDH. Our findings of downregulated BIM and higher BCL-2 in the thyroids of $Thrb^{PV/PV}Kras^{G12D}$ mice indicate that the synergistic signaling of $KRAS^{G12D}$ and TRβPV mutants led to increased proliferation and decreased apoptosis through up-regulation of MYC.

Previously, we have shown that β-catenin was activated in the thyroid tumors of $Thrb^{PV/PV}$ mice [10]. To ascertain whether β-catenin signaling was affected in the thyroid tumor progression of $Thrb^{PV/PV}Kras^{G12D}$ mice, we evaluated the protein abundance of nuclear β-catenin in mice with different genotypes by immunohistochemistry (Figure 9*B-I*). The thyroid of WT mice shows the usual flattened nuclei in the wall of the follicles with no detectable signal for β-catenin (panel *b*). The thyroid of the $Kras^{G12D}$ mice showed a more cellular follicle with many nuclei in a double layer of adjacent follicle nuclei and little detectable β-catenin. Thyroid tumors of $Thrb^{PV/PV}$ mice showed extensive adenomatous hyperplasia with some degree of cellular heterogeneity as to size and shape and similarly showed heterogeneity in the intensity of the nuclear β-catenin signal (panel *f*, Figure 9*B-I*). However, the thyroid tumors of $Thrb^{PV/PV}Kras^{G12D}$ mice showed uniform high cellularity and the nuclei showed homogeneously high levels of nuclear β-catenin (panel *h*, Figure 9*B-I*). Panels *a*, *c*, *e*, and *g* are the corresponding negative controls in which no primary antibodies were used. We further counted the cells positively stained with anti–β-catenin antibodies in the nuclei of thyroids in mice with four genotypes (Figure 9*B-II*). We found that 3.4-fold (bar 3 *vs* bar 1) and 5.3-fold (bar 4 *vs* bar 1) more cells were stained with anti–β-catenin antibodies in the thyroid of $Thrb^{PV/PV}$ and $Thrb^{PV/PV}Kras^{G12D}$ mice, respectively, than in the WT mice. These results represented that an additional 1.6-fold more β-catenin was present in the nuclei of thyroids of $Thrb^{PV/PV}Kras^{G12D}$ mice than in $Thrb^{PV/PV}$ mice. These findings indicate the contributions of increased activation of β-catenin in promoting thyroid carcinogenesis of $Thrb^{PV/PV}Kras^{G12D}$ mice.

Discussion

Association studies have indicated that mutations of *PIK3CA*, *AKT1*, *PTEN*, *CTNNB1*, *RAS*, and *BRAF* are common in anaplastic thyroid cancer [1]. These prevalent mutations suggest that the activation of PI3K-AKT, MAPK, and β-catenin signaling are critical in the development of undifferentiated thyroid cancer. Of these three major signaling pathways, it is still unknown which is essential to bring about dedifferentiated thyroid cancer. Studies from mouse models indicated that activated mutation of the *Kras* gene alone did not induce thyroid cancer. Simultaneous activation of the PI3K (through deletion of the *Pten* gene) and KRAS signaling led to only differentiated follicular thyroid carcinoma [2]. These findings suggest that additional genetic events are needed for the dedifferentiation to occur. In the present studies, we introduced $Kras^{G12D}$ mutation into $Thrb^{PV/PV}$ mice in which PI3K-AKT and β-catenin signaling are activated, leading to undifferentiated thyroid cancer [8,10,27,28]. Consistent with findings by Miller et al. [2], we found that mice harboring the activated $Kras^{G12D}$ mutation alone showed no signs of thyroid cancer. Remarkably, $Thrb^{PV/PV}$ mice harboring the activated $Kras^{G12D}$ mutation developed undifferentiated thyroid cancer. These findings suggest that cross talks of the activated KRAS pathway with the activated PI3K-AKT and β-catenin signaling mediated by TRβPV induced dedifferentiated thyroid cancer. *THRB* gene mutations

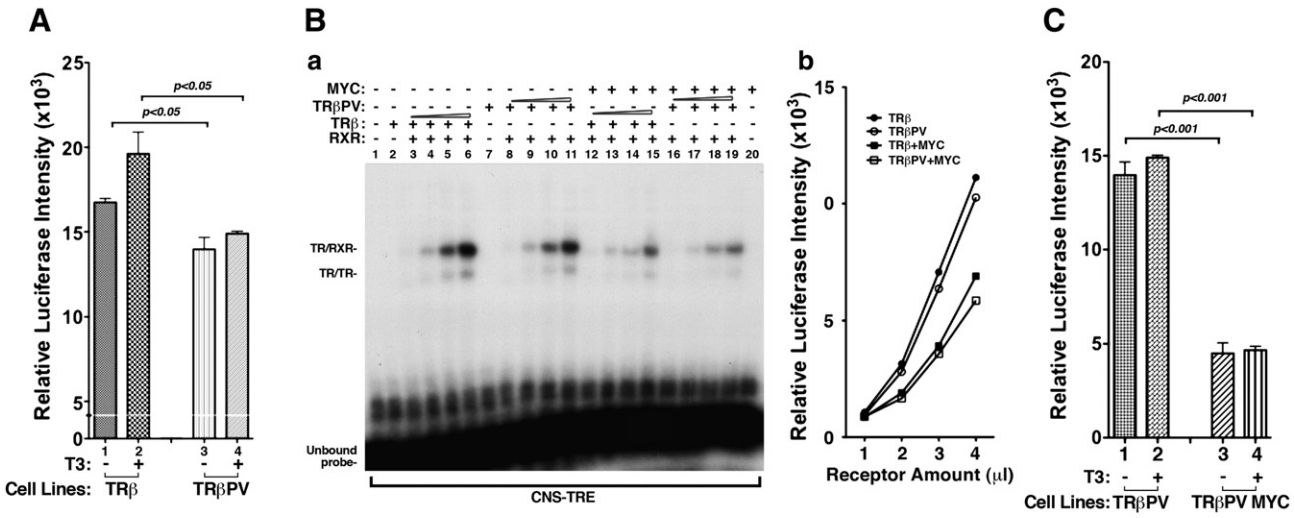

Figure 8. MYC together with TRβPV suppresses the activities of *Pax8* enhancer element. (A) Comparison of luciferase reporter activities mediated by *Pax8* upstream enhancer reporter in the absence or presence of T3 in rat thyroid pccl3 cells stably expressing TRβ (bars 1 and 2) or TRβPV (bars 3 & 4). (B-a) Binding of TRβ or TRβPV to the CNS-TRE in the absence (lanes 2-11) or presence (lanes12-19) of MYC. Electrophoretic mobility gel shift assay was carried as described in the Material and Methods section. Lanes are as marked. (B-b) Quantification of the band intensities of the TR/RXR heterodimers is shown in A-a. (C) T3/TRβ-induced reporter activity was markedly reduced in the presence of overexpressed MYC. Luciferase gene reporter assays were performed using the CNS87 element luciferase reporter in rat thyroid pccl3 cells stably expressing TRβPV alone or with both TRβPV and MYC.

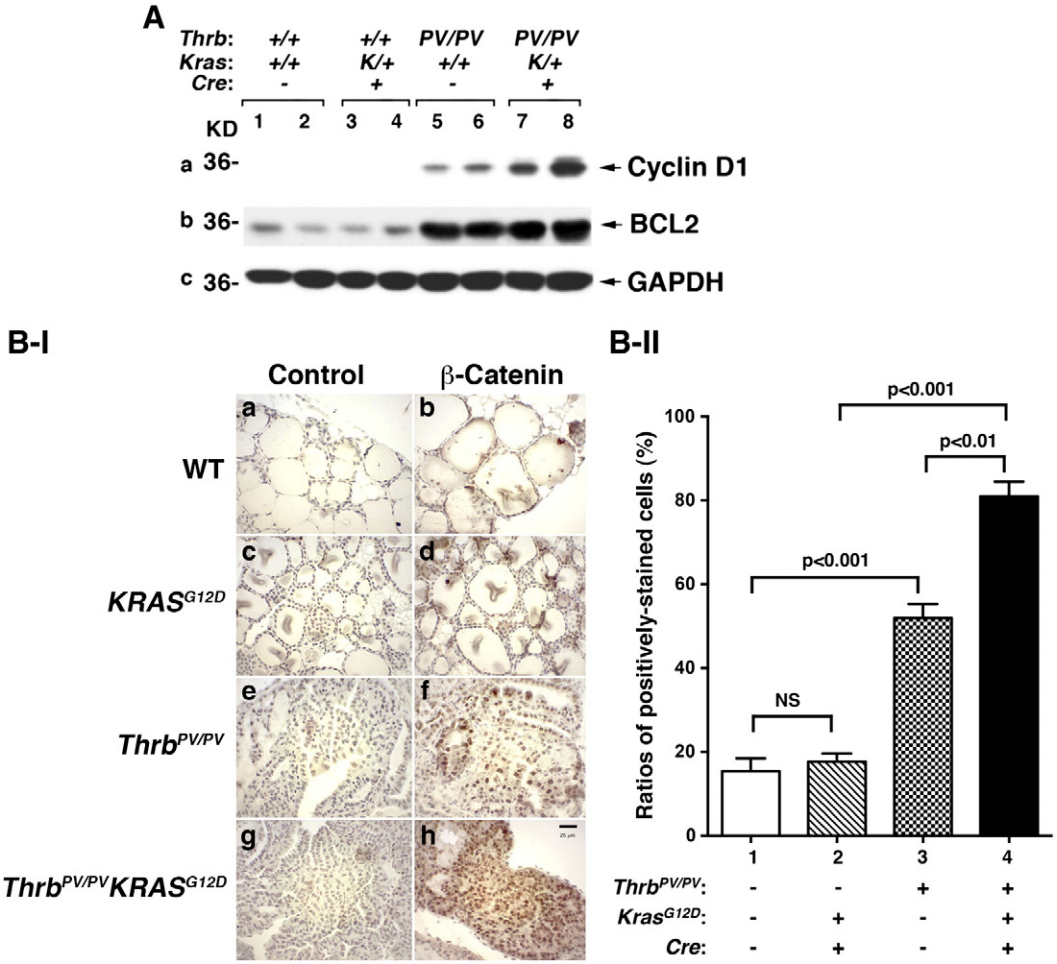

Figure 9. Increased protein abundance of key cellular regulators to promote thyroid tumor progression of $Thrb^{PV/PV}Kras^{G12D}$ mice. (A) Western blot analysis of cyclin D1 and BCL-2 with GAPDH as loading control. Representative results from two mice are shown and the genotypes are marked. (B) Increased nuclear localization of β-catenin in thyroid tumors of $Thrb^{PV/PV}Kras^{G12D}$ mice. (B-I) Immunohistochemical analysis of β-catenin in thyroid of four genotypes, as marked, was carried out as described in the Materials and Methods section. Highly elevated β-catenin was apparent in the tumor nuclei of $Thrb^{PV/PV}Kras^{G12D}$ mice. (B-II) Quantitative analysis of thyroid cells positively stained with anti–β-catenin bodies. The β-catenin–positive cells were counted by using NIH ImageJ software (Wayne Rasband, National Institutes of Health, Bethesda, MD). All data are expressed as mean ± SEM (n = 3). Significant differences between groups were calculated using ANOVA test with the use of GraphPad Prism 5 (GraphPad Software, Inc., San Diego, CA). $P < .05$ is considered statistically significant.

are rare, but case studies have reported patients with thyroid cancer [29–34]. Thousands of rare mutations have been identified in the human genome. Our observations that $KRAS^{G12D}$ together with TRβPV promoted the development of undifferentiation of thyroid cancer in mice make it possible that the cross signaling of common mutation and rare genetic event affect the progression of cancer. Their interaction may explain the heterogeneity of human cancer in the population.

To understand how the activated KRAS signaling collaborated with the TRβPV oncogenic events, thus leading to dedifferentiated thyroid cancer, we first considered the possible contribution of the elevated TSH to the dedifferentiated phenotype of $Thrb^{PV/PV}Kras^{G12D}$ mice. However, as shown in Figure 2*A*, there were no significant differences in the serum TSH levels between $Thrb^{PV/PV}$ mice and $Thrb^{PV/PV}Kras^{G12D}$ mice. Thus, TSH is unlikely to play a major role in the aggressive undifferentiated phenotype detected in $Thrb^{PV/PV}Kras^{G12D}$ mice. Given the absence of differences in serum thyroid hormone levels between $Thrb^{PV/PV}$ mice and $Thrb^{PV/PV}Kras^{G12D}$ mice, we also ruled out the possibility that thyroid hormone levels contributed to the aggressive undifferentiated thyroid cancer in $Thrb^{PV/PV}Kras^{G12D}$ mice. This notion is consistent with observations that the $Kras^{G12D}$ mutation alone in the thyroid of $Kras^{G12D}$ mice had no effect on the pituitary-thyroid axis, as shown in our present studies (see Figure 2) as well as in the studies reported by Miller et al. [2]. In addition, mice with the activated *RAS* mutation alone failed to induce thyroid cancers even in the presence of an elevated TSH level induced by propylthiouracil (PTU) for 20 weeks [3]. These findings demonstrated that not TSH but other oncogenic events were responsible for the aggressive undifferentiated thyroid carcinogenesis of $Thrb^{PV/PV}Kras^{G12D}$ mice.

MYC is one key oncogene that could play a critical role in the development of undifferentiated thyroid cancer of $Thrb^{PV/PV}Kras^{G12D}$ mice. We found that it was highly upregulated and, more importantly, tightly inversely correlated with the loss of the differentiation markers PAX8 and TTF1 (Figure 6*A*) in the anaplastic foci. Furthermore, using

rat thyroid pccl3 cells, we found that co-expression of $KRAS^{G12D}$ and TRβPV upregulated the levels of MYC at both the mRNA and protein levels (Figure 7). Although it is not yet clear how MYC was upregulated in the anaplastic tumors of $Thrb^{PV/PV}Kras^{G12D}$ mice, up-regulation of MYC by $KRAS^{G12D}$/TRβPV in the rat thyroid pccl3 cell line and the tight inverse association with PAX8 and TTF1 lead us to argue for the critical involvement of MYC in the induction of undifferentiated thyroid tumors in $Thrb^{PV/PV}Kras^{G12D}$ mice. This postulate is consistent with other studies that support MYC's key role in the differentiation process. MYC has been recognized as one of the most highly amplified oncogenes in human cancers [35]. Cell differentiation leads to down-regulation of the *MYC* expression, and overexpression of MYC results in the dedifferentiation phenotype [36]. Overexpressed MYC is also known to inhibit *Ras*-mediated differentiation by blocking c-Jun up-regulation [37] (Supplemental Figure S2). MYC also plays a key role in reprogramming human somatic cells to pluripotent stem cells [38,39]. In the above studies, however, the mechanisms by which MYC induces dedifferentiation were not clearly elucidated. In the present studies, we uncovered one mechanism by which MYC could act to participate in the induction of dedifferentiated thyroid cancer of $Thrb^{PV/PV}Kras^{G12D}$ mice through the repression of one of the differentiation transcription factors. Molecular analyses showed that TRβPV, which does not bind T3, repressed the *Pax8* gene expression. This repression was further augmented by MYC, leading to added repression in the *Pax8* transcription. At present, we could not rule out the possibility that MYC could repress the expression of the *Pax8* gene through other mechanisms independent of PV. However, our data could explain the *in vivo* findings that the *Pax8* mRNA level was less than that in WT mice, $Kras^{G12D}$ mice, and $Thrb^{PV/PV}$ mice (Figure 5*D*). While mutations of the *THRβ* gene are rare in human thyroid cancer [29–34,40], the collaboration of MYC with TRβ mutants to suppress the expression of the *Pax8* gene has yet to be uncovered. However, our findings exemplified how MYC could collaborate with other transcription factors and oncogenes to suppress the expression of the *Pax8* gene and thereby could participate in the induction of the dedifferentiation process. In line with our findings, others have shown that MYC expressed in transgenic mice triggers aggressive mammary tumorigenesis by collaborating with a KRAS mutation [41].

The up-regulation of MYC in the dedifferentiated thyroid cancer of $Thrb^{PV/PV}Kras^{G12D}$ mice provides insight into a potential therapeutic intervention. MYC is known to be essential in the maintenance of established tumors [42,43]. *In vitro* knockdown of MYC in established cancer cell lines reduces cell proliferation and, in some instances, induces apoptosis [44,45]. In transgenic mouse models with inducible *MYC* expression, established tumors regress upon withdrawal of ectopic expressed MYC. These observations suggest that MYC plays a role in tumor maintenance, and once established, these tumors are addicted to MYC for maintaining tumor phenotypes [46]. Studies using mice harboring an activated $Kras^{G12D}$ mutation showed that the blockade of MYC functions through systematic induction of a dominant-negative *MYC* allele resulted in the regression of lung carcinomas and pancreatic carcinomas [42]. Investigations have further shown that targeting MYC transcription functions by disruption of chromatin-dependent signal transduction could be effective as a therapeutic strategy. Indeed, a potent, selective small-molecule inhibitor of BET bromodomains, JQ1, was developed [47]. The efficacy of JQ1 was demonstrated in producing potent antiproliferative effects and cellular senescence in murine models of multiple myeloma [48,49]. Therefore, inhibiting MYC functions by small inhibitors could be a novel potential therapeutic strategy in the treatment of undifferentiated thyroid carcinoma. Thus, the $Thrb^{PV/PV}Kras^{G12D}$ mouse offers an opportunity not only to further elucidate the role of the KRAS in the initiation of undifferentiated thyroid cancer but also to further test novel therapeutic targets as an intervention for anaplastic thyroid cancer.

Supplementary data to this article can be found online at http://dx.doi.org/10.1016/j.neo.2014.08.003.

References

[1] Nikiforov YE and Nikiforova MN (2011). Molecular genetics and diagnosis of thyroid cancer. *Nat Rev Endocrinol* **7**(10), 569–580.

[2] Miller KA, Yeager N, Baker K, Liao XH, Refetoff S, and Di Cristofano A (2009). Oncogenic Kras requires simultaneous PI3K signaling to induce ERK activation and transform thyroid epithelial cells in vivo. *Cancer Res* **69**(8), 3689–3694.

[3] Franco AT, Malaguarnera R, and Refetoff S, et al (2011). Thyrotrophin receptor signaling dependence of Braf-induced thyroid tumor initiation in mice. *Proc Natl Acad Sci U S A* **108**(4), 1615–1620.

[4] Kaneshige M, Kaneshige K, and Zhu X, et al (2000). Mice with a targeted mutation in the thyroid hormone beta receptor gene exhibit impaired growth and resistance to thyroid hormone. *Proc Natl Acad Sci U S A* **97**(24), 13209–13214.

[5] Suzuki H, Willingham MC, and Cheng SY (2002). Mice with a mutation in the thyroid hormone receptor β gene spontaneously develop thyroid carcinoma: a mouse model of thyroid carcinogenesis. *Thyroid* **12**(11), 963–969.

[6] Parrilla R, Mixson AJ, McPherson JA, McClaskey JH, and Weintraub BD (1991). Characterization of seven novel mutations of the c-erbA beta gene in unrelated kindreds with generalized thyroid hormone resistance. Evidence for two "hot spot" regions of the ligand binding domain. *J Clin Invest* **88**(6), 2123–2130.

[7] Hou P, Liu D, and Shan Y, et al (2007). Genetic alterations and their relationship in the phosphatidylinositol 3-kinase/Akt pathway in thyroid cancer. *Clin Cancer Res* **13**(4), 1161–1170.

[8] Furuya F, Hanover JA, and Cheng SY (2006). Activation of phosphatidylinositol 3-kinase signaling by a mutant thyroid hormone β receptor. *Proc Natl Acad Sci U S A* **103**(6), 1780–1785.

[9] Lu C, Zhao L, Ying H, Willingham MC, and Cheng SY (2010). Growth activation alone is not sufficient to cause metastatic thyroid cancer in a mouse model of follicular thyroid carcinoma. *Endocrinology* **151**(4), 1929–1939.

[10] Guigon CJ, Zhao L, Lu C, Willingham MC, and Cheng SY (2008). Regulation of β-catenin by a novel nongenomic action of thyroid hormone beta receptor. *Mol Cell Biol* **28**(14), 4598–4608.

[11] Jackson EL, Willis N, Mercer K, Bronson RT, Crowley D, Montoya R, Jacks T, and Tuveson DA (2001). Analysis of lung tumor initiation and progression using conditional expression of oncogenic K-ras. *Genes Dev* **15**(24), 3243–3248.

[12] Kusakabe T, Kawaguchi A, Kawaguchi R, Feigenbaum L, and Kimura S (2004). Thyrocyte-specific expression of Cre recombinase in transgenic mice. *Genesis* **39**(3), 212–216.

[13] Furumoto H, Ying H, Chandramouli GV, Zhao L, Walker RL, Meltzer PS, Willingham MC, and Cheng SY (2005). An unliganded thyroid hormone β receptor activates the cyclin D1/cyclin-dependent kinase/retinoblastoma/E2F pathway and induces pituitary tumorigenesis. *Mol Cell Biol* **25**(1), 124–135.

[14] Zhu XG, McPhie P, and Cheng SY (1997). Differential sensitivity of thyroid hormone receptor isoform homodimers and mutant heterodimers to hormone-induced dissociation from deoxyribonucleic acid: its role in dominant negative action. *Endocrinology* **138**(4), 1456–1463.

[15] Zhao L, Zhu X, Won Park J, Fozzatti L, Willingham M, and Cheng SY (2012). Role of TSH in the spontaneous development of asymmetrical thyroid carcinoma in mice with a targeted mutation in a single allele of the thyroid hormone-β receptor. *Endocrinology* **153**(10), 5090–5100.

[16] Nitsch R, Di Dato V, di Gennaro A, de Cristofaro T, Abbondante S, De Felice M, Zannini M, and Di Lauro R (2010). Comparative genomics reveals a functional thyroid-specific element in the far upstream region of the *PAX8* gene. *BMC Genomics* **11**, 306.

[17] Rivas M and Santisteban P (2003). TSH-activated signaling pathways in thyroid tumorigenesis. *Mol Cell Endocrinol* **213**(1), 31–45.

[18] Nonaka D, Tang Y, Chiriboga L, Rivera M, and Ghossein R (2008). Diagnostic utility of thyroid transcription factors Pax8 and TTF-2 (FoxE1) in thyroid epithelial neoplasms. *Mod Pathol* **21**(2), 192–200.
[19] Fabbro D, Di Loreto C, Beltrami CA, Belfiore A, Di Lauro R, and Damante G (1994). Expression of thyroid-specific transcription factors TTF-1 and PAX-8 in human thyroid neoplasms. *Cancer Res* **54**(17), 4744–4749.
[20] Shachaf CM, Kopelman AM, and Arvanitis C, et al (2004). MYC inactivation uncovers pluripotent differentiation and tumour dormancy in hepatocellular cancer. *Nature* **431**(7012), 1112–1117.
[21] Henriksson M and Luscher B (1996). Proteins of the Myc network: essential regulators of cell growth and differentiation. *Adv Cancer Res* **68**, 109–182.
[22] Kurihara T, Ikeda S, and Ishizaki Y, et al (2004). Immunohistochemical and sequencing analyses of the Wnt signaling components in Japanese anaplastic thyroid cancers. *Thyroid* **14**(12), 1020–1029.
[23] Smallridge RC, Marlow LA, and Copland JA (2009). Anaplastic thyroid cancer: molecular pathogenesis and emerging therapies. *Endocr Relat Cancer* **16**(1), 17–44.
[24] Reynolds C, Roderick JE, and Labelle JL, et al (2014). Repression of BIM mediates survival signaling by MYC and AKT in high-risk T-cell acute lymphoblastic leukemia. *Leukemia* (advance online publication 25 March 2014).
[25] Salmanidis M, Brumatti G, and Narayan N, et al (2013). Hoxb8 regulates expression of microRNAs to control cell death and differentiation. *Cell Death Differ* **20**(10), 1370–1380.
[26] Grandori C, Cowley SM, James LP, and Eisenman RN (2000). The Myc/Max/Mad network and the transcriptional control of cell behavior. *Annu Rev Cell Dev Biol* **16**, 653–699.
[27] Furuya F, Lu C, Willingham MC, and Cheng SY (2007). Inhibition of phosphatidylinositol 3-kinase delays tumor progression and blocks metastatic spread in a mouse model of thyroid cancer. *Carcinogenesis* **28**(12), 2451–2458.
[28] Guigon CJ, Zhao L, Willingham MC, and Cheng SY (2009). PTEN deficiency accelerates tumour progression in a mouse model of thyroid cancer. *Oncogene* **28**(4), 509–517.
[29] Kim HK, Kim D, and Yoo EH, et al (2010). A case of resistance to thyroid hormone with thyroid cancer. *J Korean Med Sci* **25**(9), 1368–1371.
[30] Ramos-Prol A, Antonia Pérez-Lázaro M, Isabel del Olmo-García M, León-de Zayas B, Moreno-Macián F, Navas-de Solis S, and Merino-Torres JF (2013). Differentiated thyroid carcinoma in a girl with resistance to thyroid hormone management with triiodothyroacetic acid. *J Pediatr Endocrinol Metab* **26**(1–2), 133–136.
[31] Xifra G, Mauri S, Gironès J, Rodriguez Hermosa JI, Oriola J, Ricart W, and Fernández-Real JM (2013). Multiple Hürthle cell adenomas in a patient with thyroid hormone resistance. *Endocrinol Diabetes Metab Case Rep* **2013**, 130032.
[32] Paragliola RM, Lovicu RM, Locantore P, Senes P, Concolino P, Capoluongo E, Pontecorvi A, and Corsello SM (2011). Differentiated thyroid cancer in two patients with resistance to thyroid hormone. *Thyroid* **21**(7), 793–797.
[33] Ünlütürk U, Sriphrapradang C, Erdoğan MF, Emral R, Güldiken S, Refetoff S, and Güllü S (2013). Management of differentiated thyroid cancer in the presence of resistance to thyroid hormone and TSH-secreting adenomas: a report of four cases and review of the literature. *J Clin Endocrinol Metab* **98**(6), 2210–2217.
[34] Weinert LS, Ceolin L, Romitti M, Camargo EG, and Maia AL (2012). Is there a role for inherited TRβ mutation in human carcinogenesis? [corrected]. *Arq Bras Endocrinol Metabol* **56**(1), 67–71.
[35] Beroukhim R, Mermel CH, and Porter D, et al (2010). The landscape of somatic copy-number alteration across human cancers. *Nature* **463**(7283), 899–905.
[36] Demeterco C, Itkin-Ansari P, Tyrberg B, Ford LP, Jarvis RA, and Levine F (2002). c-Myc controls proliferation versus differentiation in human pancreatic endocrine cells. *J Clin Endocrinol Metab* **87**(7), 3475–3485.
[37] Vaqué JP, Fernández-García B, and Garcia-Sanz P, et al (2008). c-Myc inhibits Ras-mediated differentiation of pheochromocytoma cells by blocking c-Jun up-regulation. *Mol Cancer Res* **6**(2), 325–339.
[38] Park IH, Zhao R, and West JA, et al (2008). Reprogramming of human somatic cells to pluripotency with defined factors. *Nature* **451**(7175), 141–146.
[39] Takahashi K and Yamanaka S (2006). Induction of pluripotent stem cells from mouse embryonic and adult fibroblast cultures by defined factors. *Cell* **126**(4), 663–676.
[40] Joseph B, Ji M, Liu D, Hou P, and Xing M (2007). Lack of mutations in the thyroid hormone receptor (TR) α and β genes but frequent hypermethylation of the *TRβ* gene in differentiated thyroid tumors. *J Clin Endocrinol Metab* **92**(12), 4766–4770.
[41] D'Cruz CM, Gunther EJ, and Boxer RB, et al (2001). c-MYC induces mammary tumorigenesis by means of a preferred pathway involving spontaneous Kras2 mutations. *Nat Med* **7**(2), 235–239.
[42] Soucek L, Whitfield J, and Martins CP, et al (2008). Modelling Myc inhibition as a cancer therapy. *Nature* **455**(7213), 679–683.
[43] Soucek L, Whitfield JR, Sodir NM, Massó-Vallés D, Serrano E, Karnezis AN, Swigart LB, and Evan GI (2013). Inhibition of Myc family proteins eradicates KRas-driven lung cancer in mice. *Genes Dev* **27**(5), 504–513.
[44] Koh CM, Gurel B, and Sutcliffe S, et al (2011). Alterations in nucleolar structure and gene expression programs in prostatic neoplasia are driven by the MYC oncogene. *Am J Pathol* **178**(4), 1824–1834.
[45] Wang H, Mannava S, Grachtchouk V, Zhuang D, Soengas MS, Gudkov AV, Prochownik EV, and Nikiforov MA (2008). c-Myc depletion inhibits proliferation of human tumor cells at various stages of the cell cycle. *Oncogene* **27**(13), 1905–1915.
[46] Arvanitis C and Felsher DW (2006). Conditional transgenic models define how MYC initiates and maintains tumorigenesis. *Semin Cancer Biol* **16**(4), 313–317.
[47] Filippakopoulos P, Qi J, and Picaud S, et al (2010). Selective inhibition of BET bromodomains. *Nature* **468**(7327), 1067–1073.
[48] Delmore JE, Issa GC, and Lemieux ME, et al (2011). BET bromodomain inhibition as a therapeutic strategy to target c-Myc. *Cell* **146**(6), 904–917.
[49] Loven J, Hoke HA, and Lin CY, et al (2013). Selective inhibition of tumor oncogenes by disruption of super-enhancers. *Cell* **153**(2), 320–334.